Title

Evaluation of Bi-layer Silk Fibroin Grafts for Inlay Vaginoplasty in a Rat Model

Authors

Nguyen, Travis
Gundogdu, Gokhan
Bottini, Christina
et al.

Publication Date

2024-05-31

DOI

10.1007/s13770-024-00653-1

Peer reviewed

Evaluation of Bi-layer Silk Fibroin Grafts for Inlay Vaginoplasty in a Rat Model

Running Title: Vaginal Reconstruction with Silk Fibroin Grafts

Travis Nguyen, B.Sc.[2#], Gokhan Gundogdu, M.D.[1#], Christina Bottini, B.Sc.[2], Ambika K. Chaudhuri, B.Sc.[2], Joshua R. Mauney, Ph.D.[1,2,*]

[1]Department of Urology, University of California, Irvine, Orange, CA, USA.

[2]Department of Biomedical Engineering, University of California, Irvine, Irvine, CA, USA.

[#]Equal contribution.

[*]Corresponding author: Joshua R. Mauney, Ph.D., University of California, Irvine, Departments of Urology and Biomedical Engineering, Building 55, 101 The City Drive South., Rm. 300, Orange, CA 92868, USA; Phone: +001-714-456-6782; Fax: +001-888-378-4358; email: mauneyj@hs.uci.edu

Abstract

Background: Autologous tissues derived from bowel, buccal mucosa and skin are primarily used to repair or replace diseased vaginal segments as well as create neovaginas for male-to-female transgenders. These grafts are often limited by scarce tissue supply, donor site morbidity and post-operative complications. Bi-layer silk fibroin (BLSF) biomaterials represent potential alternatives for vaginoplasty given their structural strength and elasticity, low immunogenicity, and processing flexibility. The goals of the current study were to assess the potential of acellular BLSF scaffolds for vaginal tissue regeneration in respect to conventional small intestinal submucosal (SIS) matrices in a rat model of vaginoplasty. **Methods:** Inlay vaginoplasty was performed with BLSF and SIS scaffolds (N=21 per graft) in adult female rats for up to 2 months of implantation. Nonsurgical controls (N=4) were investigated in parallel. Outcome analyses included histologic, immunohistochemical and histomorphometric evaluations of wound healing patterns; μ–computed tomography (CT) of vaginal continuity; and breeding assessments. **Results:** Animals in both scaffold cohorts exhibited 100% survival rates with no severe post-operative complications. At 2 months post-op, μ–CT analysis revealed normal vaginal anatomy and continuity in both graft groups similar to controls. In parallel, BLSF and SIS grafts also induced comparable constructive remodeling patterns and were histologically equivalent in their ability to support formation of vascularized vaginal neotissues with native tissue architecture, however with significantly less smooth muscle content. Vaginal tissues reconstructed with both implants were capable of supporting copulation, pregnancy and similar amounts of live births. **Conclusions:** BLSF biomaterials represent potential "off-the-shelf" candidates for vaginoplasty.

Keywords: vagina, silk fibroin, vaginoplasty, biomaterial

1. Introduction

Pediatric and adult disorders of the vagina including vaginal atresia, adrenal hyperplasia, cloacal malformations, malignancy and stenosis can significantly compromise female sexual function, fertility and quality of life [1-3]. Autologous tissue grafts derived from bowel or buccal mucosa as well as musculocutaneous and cutaneous flaps are primarily used to replace developmentally absent or diseased vaginal segments when conservative management such as dilation or progressive traction fail to restore organ caliber and length [4-6]. In addition, penile inversion vaginoplasty with autologous penile skin represents the gold standard approach for neovagina creation during transgender feminization procedures [7]. Despite widespread deployment of autologous tissues for vaginal reconstruction, these grafts are often limited by scarce tissue supply, donor site morbidity and postoperative complications such as strictures, fistula formation, and adhesions [8-12]. Given the drawbacks associated with patient-derived tissues for vaginoplasty, new biological substitutes are needed which can promote functional vaginal tissue regeneration in the absence of adverse side effects.

Tissue engineered grafts utilizing acellular and cell-seeded, biodegradable biomaterials have been investigated as alternatives to autologous tissues for vaginal repair [13]. These technologies have been explored in a number of preclinical animal models and human trials and have included patches and conduits composed of natural scaffolds such as decellularized tissues from vagina, bladder and intestinal submucosa (SIS) as well as synthetic polyester [14-23]. In general, cell-seeded grafts populated with ex vivo expanded, patient-derived epithelial and smooth muscle cells or stem cell populations have generated superior functional outcomes in comparison

to acellular counterparts, supporting the formation of vaginal neotissues with native architecture and in some cases copulation [16,19,24,25]. In contrast, conventional acellular scaffolds derived from decellularized tissues and synthetic polyesters are prone to graft contracture and luminal collapse with fibrotic tissue formation routinely observed at implant sites [17,19]. Nevertheless, cell-free scaffolds offer distinct advantages over cell-seeded matrices for vaginal tissue engineering such as the lack of secondary surgical procedures to procure cells for construct incorporation, dispensability of tissue culture facilities for ex vivo cell isolation and expansion, and "off-the-shelf" utility.

Previous research from our laboratory suggests that bi-layer silk fibroin (BLSF) biomaterials may serve as potential acellular platforms for reconstruction of vaginal defects [26]. In particular, these protein-based matrices exhibit tunable structural and mechanical properties, low immunogenicity and have been shown to facilitate repair of various hollow organs including the bladder, ureter, urethra, esophagus and trachea in preclinical settings [27-31]. The unique architecture of BLSF grafts allows for maintenance of organ continuity at implant sites via a fluid-tight film layer, while a porous foam compartment facilitates host tissue ingrowth and neotissue formation [32]. Therefore, the goals of the current study were to assess the efficacy of acellular BLSF scaffolds for vaginal tissue regeneration and compare functional and histological outcomes to conventional SIS matrices in a rat model of inlay vaginoplasty.

2. Material and Methods

2.1 Biomaterials

BLSF biomaterials were manufactured from aqueous silk fibroin solutions using established protocols [32]. Briefly, sericin-depleted, silk fibroin solutions (8% weight/volume) derived from *Bombyx mori* cocoons were dried for 48 hours at room temperature in a casting container under laminar flow to create a silk fibroin film. A 6% weight/volume silk fibroin solution was then mixed with sieved granular NaCl (500–600 μM, average crystal diameter) in a ratio of 2 g NaCl per ml of silk fibroin solution and deposited on top of the silk fibroin film. The resultant solution was allowed to undergo self-assembly and fuse to the silk fibroin film for 48 hours at 37 °C to create the BLSF matrix. NaCl was removed thereafter by rinsing the scaffold for 72 hours in distilled water. BLSF grafts were trimmed and steam sterilized in an autoclave prior to implantation. Commercially available, SIS scaffolds (Biodesign 4-Layer Tissue Graft; Cook Medical, Bloomington, IN, United States) were evaluated in parallel animal studies as points of comparison.

2.2 Study Design

All animal procedures were performed in compliance with the National Institutes of Health's Guidelines for the Care and Use of Laboratory Animals and were reviewed and approved by the University of California, Irvine Animal Care and Use Committee in accordance with protocol AUP-22-009. Forty-two adult, virgin female Sprague-Dawley rats (240-280 g, Charles River Laboratories, Charles River Laboratories, Wilmington, MA) were randomized across 2 implant groups and subjected to inlay vaginoplasty (**Fig. 1**) with either BLSF (N=21) or SIS (N=21) grafts as described below. Animals in both scaffold groups were harvested for outcome

analyses at 1 day (N=3 per implant), 1 week (N=4 per implant), 1 month (N=5 per implant) and 2 months (N=5 per implant) post-operatively to determine longitudinal wound healing and host tissue responses. Nonsurgical controls (NSC) (N=4) were analyzed in parallel and served as positive controls. In addition, breeding experiments were carried out with rats from both matrix groups (N=4 per implant) 2 months following vaginal reconstruction to assess copulation and delivery functions as detailed in subsequent sections.

2.3 Inlay vaginoplasty

General anesthesia was induced and maintained by inhalation with 2–4% isoflurane. Rats were placed in a supine position and the perineum was shaved and sterilely draped. The vaginal introitus was retracted with stay sutures and a full thickness defect (10 x 5 mm^2) was created in the posterior vaginal wall 1-2 mm proximal from the orifice. A graft of equal size was incorporated into the defect area with 7-0 polyglactin interrupted sutures. Nonabsorbable 7-0 polypropylene sutures were placed along the anastomotic perimeter for delineation of matrix borders following sacrifice. Postoperative pain control was accomplished by a single subcutaneous injection of 1.2 mg/kg Buprenorphine SR (ZooPharm, Laramie, WY, United States) immediately following surgery with subcutaneous injections of 2.5 mg/kg Banamine (Merck Animal Health, Kenilworth, NJ, United States) carried out for 3 days post-operatively. In addition, Enrofloxacin (Baytril®100; Bayer Healthcare LLC, KA, United States) was administered subcutaneously before surgery and continued for 2 postoperative days to prevent infection. At selected timepoints, rats were subjected to imaging and/or breeding analyses and then euthanized by CO_2 asphyxiation for histological and immunohistochemical (IHC) assessments.

2.4 Micro–computed tomography

Micro–computed tomography (μCT) was performed on NSC (N = 4) and implant groups (N=5 per scaffold) at 2 months following vaginoplasty to evaluate organ continuity and structure. Under isofluorane anesthesia, rats were placed in the supine position and a purse string was placed at the skin level of the vaginal introitus using a 5-0 nonabsorbable suture. A 14 gauge IV cannula was then introduced into the vagina and secured with a purse string. Contrast medium (Omnipaque 300; GE Healthcare Inc., Marlborough, MA, USA) diluted with 1:1 saline was infused into the vagina followed by cannula removal and closure of the vaginal orifice. Lower abdomen scans were acquired with a Siemens Inveon(r) Multi-Modality System PET/CT (Siemens Healthcare, Erlangen, Germany) and 3-D images of the vaginal lumen were created using Inveon Research Workplace (Siemens Healthcare) 3D Analysis software.

2.5 Breeding and live birth assessments

Following 2 months of scaffold implantation, rats subjected to vaginal repair with BLSF and SIS matrices (N=4 per matrix) were evaluated for their ability to copulate, achieve pregnancy and deliver live births. Each female was co-housed with one male rat for 2 weeks to allow for mating. Pregnancy was confirmed by monitoring abdominal distension, weight and breast development over the gestational period. The rate of pregnancy and number of live births were quantified across groups.

2.6 Histologic, immunohistochemical, and histomorphometric analyses

Following euthanasia, reconstructed vaginal segments (N=3-5 per timepoint) as well as NSC replicates (N=4) were formalin fixed for 12 hours, dehydrated in graded alcohols and embedded in paraffin for sectioning. Specimens (5 μm) were stained with Masson's trichrome (MTS), digitally imaged and total collagen content was determined in control and implant regions with ImageJ software (version 1.47) using published methods to quantify blue-stained color elements representative of collagen deposition [28]. Total collagen content was calculated as the percentage of blue-stained area per total field area and normalized to NSC levels. IHC analyses were carried out on parallel tissue sections following antigen retrieval (pH 6.0, 10 mm sodium citrate buffer) and incubation in phosphate-buffered saline with 0.3% Triton X-100, 5% fetal bovine serum, and 1% bovine serum albumin for 1 hour at room temperature. Sections were probed at 4ºC overnight with primary antibodies including anti-α-smooth muscle actin (SMA) (1:200 dilution; Sigma-Aldrich, St. Louis, MO), anti-SM22α (1:200 dilution, Abcam, Cambridge, MA), anti-pan-cytokeratin (CK) (1:150 dilution; Dako, Carpinteria, CA), anti-CD31 (1:100 dilution; Abcam) and vimentin (1:100 dilution; Abcam). Samples were then stained with species-matched Alexa Fluor 647 and 488-conjugated secondary antibodies (Thermo Fisher Scientific) and nuclear counterstained with 4′, 6-diamidino-2-phenyllindole (DAPI). Specimen visualization was performed with an Axioplan-2 microscope (Carl Zeiss MicroImaging, Thornwood, NY) and representative fields were acquired with Axiovision software (version 4.8). Negative controls were stained in parallel with secondary antibodies alone and generated no detectable signal above background. Histomorphometric evaluations were performed on NSC (N=4) and neotissues (N=3-5 per timepoint) utilizing 6-8 independent microscopic fields (10X magnification). Stained

elements were quantified from specimen cross-sections with published protocols using ImageJ software [30]. Relative immunoreactivities of α-SMA, SM22α, vimentin and pan-CK were presented as the percentage of stained area per total field area relative to NSC values. Vascular densities were determined similarly by quantifying the number of CD31+ vessels per target field area.

2.7 Statistical evaluations

Multi-group comparisons were carried out with the Kruskal Wallis test followed by pairwise evaluations with the post hoc Dunn's test. For two group comparisons of live birth data, the Mann-Whitney U test was utilized. For all statistical tests, $p<0.05$ was defined as significant. All quantitative data were displayed as means ± standard deviation (SD).

3. Results

Animals in both implant cohorts exhibited 100% survival rates until scheduled euthanasia. In addition, there was no evidence of serve intraoperative or postoperative complications following vaginoplasty in either group over the course of the study, however mild hematomas were detected at the reconstructed sites in 3 rats prior to sacrifice (BLSF: N=2, 1 day post-op; SIS: N=1, 2 months post-op). At 2 months post-op, μCT imaging revealed normal vaginal anatomy in both graft groups similar to NSC with no signs of contrast extravasation, strictures or fistula formation (**Fig. 2**). These observations were confirmed during parallel necropsy evaluations wherein patent vaginal canals with wide calibers were evident in both BLSF and SIS groups. Residual scaffold fragments

were found in the vaginal lumens of both biomaterial cohorts up to 1 month post-reconstruction, but were undetectable by the 2 month timepoint. Host tissue ingrowth was apparent throughout the original reconstructed areas in both experimental groups by 1 week post-op with negligible tissue contraction detected between proximal/distal or lateral marking sutures at harvest (**Fig. 2**). These results demonstrate that BLSF grafts are capable of supporting consolidation of focal vaginal defects and restoring organ continuity to similar extents as conventional SIS matrices.

Characterization of host tissue responses and wound healing outcomes were performed on control and implant groups across the study period with histologic, IHC and histomorphometric analyses (**Fig. 3 and 4**). Baseline evaluations of vaginal cross-sections in NSC revealed native tissue architecture composed of a luminal, stratified squamous, keratinizing epithelium with pan-CK expression, an extra-cellular matrix (ECM)-rich lamina propria populated with vimentin+ fibroblasts and an outer muscularis layer consisting of circular and longitudinal smooth muscle bundles displaying contractile proteins, α-SMA and SM22α. By 1 day post-op, MTS evaluations demonstrated that reconstructed regions in each scaffold group exhibited nascent ECM formation and were infiltrated with mononuclear inflammatory cells, neutrophils, and fibroblasts. Prominent extrusion of bulk scaffold fragments into the vaginal lumen was also observed in each group at this phase of repair. At 1 week post-op, neotissues in each experimental group had developed a vascularized lamina propria lined by a pan-CK+ stratified squamous, keratinizing epithelium similar to NSC. Transient myofibroblast differentiation was also detected in remodeling vaginal walls at this stage exemplified by significant upregulation of vimentin expression compared to NSC and co-expression of α-SMA and SM22α proteins in this population. Maturation of neotissues in each implant cohort continued to progress between 1 week and 2 months with the

formation of α-SMA+SM22α+ smooth muscle bundles coupled with a parallel decline in vimentin+myfibroblasts to baseline levels. Reconstructed tissues also displayed similar degrees of collagen content compared to NSC by 1 and 2 months post implantation. In addition, no evidence of chronic inflammatory reactions or foreign body responses were observed in either neotissue at study timepoints.

Overall, no significant differences in regenerative outcomes were found between SIS and BLSF groups suggesting vaginal wound healing patterns were conserved across these implant configurations. However, neotissues from each scaffold cohort were still underdeveloped at 2 months and displayed 25-50% smooth muscle content relative to NSC as well as significantly higher vascular densities consistent with ongoing phases of tissue remodeling. Nevertheless, breeding assessments (**Fig. 5**) revealed that animals repaired with both BLSF and SIS biomaterials were capable of copulation with 100% pregnancy rates and similar amounts of live births. These data provide evidence that BLSF grafts can promote functional vaginal tissue regeneration sufficient to support sexual intercourse and delivery of live offspring.

4. Discussion

The aims of this study were to evaluate the feasibility of acellular BLSF grafts for vaginal reconstruction and compare functional and wound healing responses to decellularized SIS biomaterials previously deployed in the clinic. Adult rats were chosen as a model species due to their low cost as well as their similarities in organ anatomy and reproductive cycle relative to humans [33]. The regenerative potential of study biomaterials was investigated in an inlay

vaginoplasty model which mimics the repair of focal vaginal defects encountered in patients following resection of urogenital malignancies [34-35] or those with severe obstetric lacerations after childbirth [36]. BLSF and SIS grafts were found to induce similar constructive remodeling patterns in patch vaginal defects and were histologically equivalent in their ability to support the formation of vascularized neotissues containing stratified squamous, keratinizing epithelia as well as smooth muscle layers. However, smooth muscle content was significantly lower in neotissues relative to NSC suggesting longer implantation periods or scaffold-mediated, delivery of pro-myogenic compounds such as platelet derived growth factor [37] may be necessary to improve smooth muscle growth. Functional evaluations of vaginas reconstructed with BLSF and SIS biomaterials confirmed their ability to support copulation and live births thus providing evidence that these matrix configurations can reestablish organ continuity sufficient for reproduction. Spontaneous, partial wound healing of full thickness vaginal defects in rats without scaffold implantation has been previously reported [38, 39]. In this setting, neotissues display re-epithelialization with altered vaginal wall biomechanics compared to non-injured controls [39]. Future investigations will compare regenerative outcomes elicited by scaffold configurations to sham-operated controls to uncouple the effects of scaffold-mediated, constructive remodeling from baseline repair mechanisms.

Currently, patients with congenital vaginal abnormalities such as Mayer-Rokitansky-Küster-Hauser Syndrome (MRKHS) as well as male-to-female transgenders require the creation of tubular neovaginas from autologous tissues to restore sexual function [40]. Decellularized tissues grafts such as SIS have been previously explored as an biomaterial substitutes for tubular vaginoplasty in MRKHS individuals, however suboptimal outcomes including relatively short

neovaginas (<7 cm for 46.4% of patients), excessive vaginal discharge and chronic bacterial infections were observed [41]. Moreover, preclinical assessments of decellularized tissue matrices for tubular vaginoplasty have also noted frequent graft contracture and luminal collapse in rodent neovaginas [17]. BLSF matrices possess a number of potential advantages relative to decellularized tissue biomaterials for the design of tubular implants for vaginoplasty. In particular, the mechanical, structural and degradative properties of BLSF scaffolds can be adjusted by manipulating processing parameters such as porogen size and silk fibroin content to create constructs with biomechanical features sufficient for maintaining hollow organ integrity [42-44]. Indeed, these matrix configurations have been previously reported to serve as urinary conduits [45] as well as facilitate functional repair of tubular defects in both the ureter and [30-31] In contrast, the physical characteristics of decellularized tissue grafts are dependent upon the attributes of the source tissue as well as decellularization protocols [46] and therefore have limited capacity to modulate structural integrity to prevent stenotic events. Future in vivo studies will investigate the efficacy of tubular BLSF grafts for neovagina formation.

In conclusion, acellular BLSF biomaterials were found to be permissive for regeneration of focal vaginal defects, producing neotissues with native-like architecture with the ability to support sexual intercourse, pregnancy and live births in a preclinical animal model. Wound healing outcomes and functional responses elicited by BLSF grafts following vaginal reconstruction were comparable to conventional SIS scaffolds. However, the high degree of processing plasticity of silk fibroin biomaterials may allow for the future creation of acellular tubular conduits for full vaginal replacement that can overcome the biomechanical limitations associated with decellularized tissue grafts. In addition, next-generation BLSF scaffold designs will also

incorporate drug delivery capabilities with the potential to facilitate targeted release of pro-myogenic agonists to improve vaginal smooth muscle formation. In summary, BLSF biomaterials represent attractive candidates for vaginoplasty and may offer a functional "off-the-shelf" alternative for the use of conventional autologous tissues for vaginal repair.

Acknowledgements

This study was supported by the National Institutes of Health Grants, R01DK131211 (Mauney) and R01DK119240 (Mauney). We also acknowledge Ms. Charlotte Morgan for technical assistance.

Author Contributions

J.M. and G.G. conceived the study and developed the experimental plan. G.G. wrote and edited the animal protocol. G.G. performed all surgical manipulations and imaging analyses as well as provided animal husbandry. J.M. fabricated the BLSF grafts. T.N., C.B., and A.C. acquired and analyzed histological, immunohistochemical, and histomorphometic data. T.N. carried out statistical analyses. J.M., G.G. and T.N. wrote the article. All authors reviewed and edited the article for conceptual and technical content. JM coordinated and supervised all aspects of the study.

Data Availability

The study datasets for the current study are available from the corresponding author on reasonable request.

Conflicts of Interest

The authors declare no conflicts of interest.

Ethical Statement

The animal studies were performed after receiving approval from the University of California, Irvine Animal Care and Use Committee in accordance with protocol AUP-22-009.

References

1. Quint EH, McCarthy JD, Smith YR. Vaginal surgery for congenital anomalies. Clin Obstet Gynecol 2010;53:115-24.
2. Kulkarni A, Dogra N, Zigras T. Innovations in the Management of Vaginal Cancer. Curr Oncol. 2022;29:3082-92.
3. Laganà AS, Garzon S, Raffaelli R, Ban Frangež H, Lukanovič D, Franchi M. Vaginal Stenosis After Cervical Cancer Treatments: Challenges for Reconstructive Surgery. J Invest Surg. 2021;34:754-755.
4. Horch RE, Hohenberger W, Eweida A, Kneser U, Weber K, Arkudas A, et al. A hundred patients with vertical rectus abdominis myocutaneous (VRAM) flap for

pelvic reconstruction after total pelvic exenteration. Int J Colorectal Dis. 2014;29:813-23.

5. Bouman MB, van Zeijl MC, Buncamper ME, Meijerink WJ, van Bodegraven AA, Mullender MG. Intestinal vaginoplasty revisited: a review of surgical techniques, complications, and sexual function. J Sex Med. 2014;11:1835-47.
6. Learner HI, Creighton SM, Wood D. Augmentation vaginoplasty with buccal mucosa for the surgical revision of postreconstructive vaginal stenosis: a case series. J Pediatr Urol. 2019;15:e1-e7.
7. Buncamper M, van der Sluis W, Van der Pas R, Özer M, Smit J, Witte B, et al. Surgical outcomes after penile inversion vaginoplasty: a retrospective study of 475 transgender women. Plastic Reconstr Surg 2016;138:999–1007.
8. Kisku S, Varghese L, Kekre A, Sudipta S, Sampath K, Mathai J, et al. Bowel vaginoplasty in children and young women: an institutional experience with 55 patients. Int Urogynecol J 2015;26:1441–48.
9. Van der Sluis W, Bouman M, Meijerink W, Elfering L, Mullender M, De Boer N, et al. Diversion neovaginitis after sigmoid vaginoplasty: endoscopic and clinical characteristics. Fertil Steril 2016;105:834–839.
10. Hensle TW, Reiley EA. Vaginal replacement in children and young adults. J Urol 1998;159:1035–38.
11. Oelschlager A, Kirby, A, Breech, L. Evaluation and management of vaginoplasty complications. Current Opinion in Obstetrics and Gynecology; 2017;29:316-321.

12. Bastu E, Akhan S, Mutlu M, Nehir A, Yumru H, Hocaoglu E, et al. Treatment of vaginal agenesis using a modified McIndoe technique: long-term follow-up of 23 patients and a literature review. Can J Plast Surg 2012;20:241-4.
13. Brownell D, Chabaud S, Bolduc S. Tissue Engineering in Gynecology. Int J Mol Sci. 2022;23:12319.
14. Sueters J, Xiao F, Roovers JP, Bouman MB, Groenman F, Maas H, et al. Creation of a decellularized vaginal matrix from healthy human vaginal tissue for potential vagina reconstruction: experimental studies. Int J Surg. 2023;109:3905-18.
15. Zhang X, Qiu J, Ding J, Hua K. Comparison of neovaginoplasty using acellular porcine small intestinal submucosa graft or Interceed in patients with Mayer–Rokitansky–Küster–Hauser syndrome. Arch Gynecol Obstet. 2019;300:1633-36.
16. Raya-Rivera AM, Esquiliano D, Fierro-Pastrana R, López-Bayghen E, Valencia P, Ordorica-Flores R, et al. Tissue-engineered autologous vaginal organs in patients: a pilot cohort study. Lancet. 2014;384:329-36.
17. Wefer J, Sekido N, Sievert K.D, Schlote N, Nunes L, Dahiya R, et al. Homologous acellular matrix graft for vaginal repair in rats: A pilot study for a new reconstructive approach. World J. Urol. 2002;20:260–63.
18. De Filippo RE, Yoo JJ, Atala A. Engineering of Vaginal Tissue in Vivo. 2003;9:301-6.
19. De Filippo RE, Bishop CE, Filho LF, Yoo JJ, Atala A. Tissue engineering a complete vaginal replacement from a small biopsy of autologous tissue. Transplantation. 2008;86:208-14.

20. Ding JX, Zhang XY, Chen LM, Hua KQ. Vaginoplasty using acellular porcine small intestinal submucosa graft in two patients with Meyer-von-Rokitansky-Küster-Hauser syndrome: a prospective new technique for vaginal reconstruction. Gynecol Obstet Invest. 2013;75:93-6.
21. Ding JX, Chen LM, Zhang XY, Zhang Y, Hua KQ. Sexual and functional outcomes of vaginoplasty using acellular porcine small intestinal submucosa graft or laparoscopic peritoneal vaginoplasty: a comparative study. Hum Reprod. 2015;30:581-9.
22. Zhang X, Liu Z, Yang Y, Yao Y, Tao Y. The clinical outcomes of vaginoplasty using tissue-engineered biomaterial mesh in patients with Mayer-Rokitansky-Küster-Hauser syndrome. Int J Surg. 2017;44:9-14.
23. Gomes TG, Agostinho M, Cardoso MC, Costa JND, Matias J. XCM Biologic Tissue Matrix xenograft and autologous micromucosa graft for vaginal reconstruction in Mayer-Rokitansky-Küster-Hauser syndrome. Arch Plast Surg. 2021;48:185-8.
24. Ho MH, Heydarkhan S, Vernet D, Kovanecz I, Ferrini MG, Bhatia NN, et al. Stimulating vaginal repair in rats through skeletal muscle-derived stem cells seeded on small intestinal submucosal scaffolds. Obstet Gynecol. 2009;114:300-9.
25. Zhang N, Qin X, Zhang J, Zhang Z, Li Y, Xie Y, et al. Bone Marrow Mesenchymal Stem Cells Accelerate the Morphological and Functional Recovery of Neovaginas. Artif Organs. 2018;42:1206-15.

26. Sack BS, Mauney JR, Estrada CR Jr. Silk Fibroin Scaffolds for Urologic Tissue Engineering. Curr Urol Rep. 2016;17:16.
27. Chung YG, Tu D, Franck D, Gil ES, Algarrahi K, Adam RM, et al. Acellular bi-layer silk fibroin scaffolds support tissue regeneration in a rabbit model of onlay urethroplasty. PLoS One. 2014;9:e91592.
28. Affas S, Schäfer FM, Algarrahi K, Cristofaro V, Sullivan MP, Yang X, et al. Augmentation Cystoplasty of Diseased Porcine Bladders with Bi-Layer Silk Fibroin Grafts. Tissue Eng Part A. 2019;25:855-66
29. Galvez C, Gundogdu G, Yang X, Costa K, Mauney JR. Evaluation of Acellular Bilayer Silk Fibroin Grafts for Onlay Tracheoplasty in a Rat Defect Model. Otolaryngol Head Neck Surg. 2019;160:310-19.
30. Gundogdu G, Okhunov Z, Cristofaro V, Starek S, Veneri F, Orabi H, et al. Evaluation of Bi-Layer Silk Fibroin Grafts for Tubular Ureteroplasty in a Porcine Defect Model. Front Bioeng Biotechnol. 2021;9:723559.
31. Gundogdu G, Morhardt D, Cristofaro V, Algarrahi K, Yang X, Costa K, et al. Evaluation of Bilayer Silk Fibroin Grafts for Tubular Esophagoplasty in a Porcine Defect Model. Tissue Eng Part A. 2021;27:103-16.
32. Seth A, Chung YG, Gil ES, Tu D, Franck D, Di Vizio D, et al. The performance of silk scaffolds in a rat model of augmentation cystoplasty. Biomaterials. 2013;34:4758-65.
33. McCracken JM, Calderon GA, Robinson AJ, Sullivan CN, Cosgriff-Hernandez E, Hakim JCE. Animal Models and Alternatives in Vaginal Research: a Comparative Review. Reprod Sci. 2021;28:1759-73.

34. Parsons JK, Tufaro A, Chang B, Schoenberg MP. Rectus abdominis vaginoplasty after anterior exenteration for urologic malignancy. Urology. 2003;61:1249-52.
35. Thomas JC, Brock JW 3rd. Vaginal substitution: attempts to create the ideal replacement. J Urol. 2007;178:1855-59.
36. Committee on Practice Bulletins–Obstetrics. ACOG practice bulletin no. 198: prevention and management of obstetric lacerations at vaginal delivery. Obstet Gynecol. 2018;132:e87-e102.
37. Wang Y, Wu T, Zhang J, Feng Z, Yin M, Mo X. A bilayer vascular scaffold with spatially controlled release of growth factors to enhance in situ rapid endothelialization and smooth muscle regeneration, Materials & Design, 2021; Volume 204, 109649, ISSN 0264-1275.
38. Ben Menachem-Zidon O, Gropp M, Ben Shushan E, Reubinoff B, Shveiky D. Systemically transplanted mesenchymal stem cells induce vascular-like structure formation in a rat model of vaginal injury. PLoS One. 2019;14:e0218081.
39. Shveiky D, Iglesia CB, Sarkar Das S, Ben Menachem-Zidon O, Chill HH, Ji H, Sandberg K. Age-associated impairments in tissue strength and immune response in a rat vaginal injury model. Int Urogynecol J. 2020;31:1435-1441.
40. Sueters J, Groenman FA, Bouman MB, Roovers JPW, de Vries R, Smit TH, et al. Tissue Engineering Neovagina for Vaginoplasty in Mayer-Rokitansky-Küster-Hauser Syndrome and Gender Dysphoria Patients: A Systematic Review. Tissue Eng Part B Rev. 2023;29:28-46.
41. Ding JX, Chen LM, Zhang XY, Zhang Y, Hua k. Sexual and functional outcomes of vaginoplasty using acellular porcine small intestinal submucosa graft or

laparoscopic peritoneal vaginoplasty: A comparative study. Hum Reprod 2015;30:581–9.

42. Kim UJ, Park J, Kim HJ, Wada M, Kaplan DL. Three-dimensional aqueous-derived biomaterial scaffolds from silk fibroin. Biomaterials. 2005;26:2775-85.
43. Wang Y, Rudym DD, Walsh A, Abrahamsen L, Kim HJ, Kim HS, et al. In vivo degradation of three-dimensional silk fibroin scaffolds. Biomaterials. 2008;29:3415-28.
44. Tu DD, Chung YG, Gil ES, Seth A, Franck D, Cristofaro V, et al. Bladder tissue regeneration using acellular bi-layer silk scaffolds in a large animal model of augmentation cystoplasty. Biomaterials. 2013;34:8681-8689.
45. Gundogdu G, Nguyen T, Hosseini Sharifi SH, Starek S, Costa K, Jones CE, et al. Evaluation of silk fibroin-based urinary conduits in a porcine model of urinary diversion. Front Bioeng Biotechnol. 2023;11:1100507.
46. Brown BN, Badylak SF. Extracellular matrix as an inductive scaffold for functional tissue reconstruction. Transl Res. 2014;163:268-285.

Figure Legends

Figure 1. Rat inlay vaginoplasty model. [**A**] Photomicrograph of BLSF graft prior to vaginal implantation. [**B**] Suture retraction of the vaginal introitus exposing the posterior vaginal wall. [**C**] Creation of vaginal defect in the posterior vagina. [**D**] Vaginal reconstruction with BLSF graft.

Figure 2. Necropsy and μCT analyses of neotissue formation and vaginal continuity. [**Top row**] Gross tissue assessments of vaginas reconstructed with BLSF or SIS grafts following 2 months of implantation in comparison to NSC. Boxed regions denote original implant site. [**Bottom row**] Representative 3-D images of vaginas in NSC and scaffold groups detailed in [A] following contrast instillation and μCT imaging.

Figure 3. Histological assessments of vaginal tissue regeneration. [**A-C**] Photomicrographs of global (top rows) and magnified (bottom rows) cross-sections of MTS-stained, vaginas in NSC [A] and in animals repaired with BLSF [B] and SIS grafts [C] at selective post-operative timepoints containing the original implant site (boxed). For panels [A-C], scale bars are 2.5 mm and 1 mm in top and bottom rows, respectively. R denotes rectum. Asterisks denote residual scaffold fragments. [**D**] Quantitation of collagen content in MTS-stained vaginal neotissues and NSC displayed in [A-C]. N=3-5 rats per group were assessed per data point. Data are displayed as means ± SD. Data from all cohorts were analyzed with Kruskal–Wallis and post hoc Dunn's tests. (*) = $p<0.05$ compared to NSC. (#) = $p>0.05$ compared to NSC.

Figure 4. Immunohistochemical and histomorphometric evaluations of vaginal neotissues and controls. [**A-B**] Photomicrographs of vaginal protein expression in NSC and regenerated tissues following vaginoplasty with BLSF [A] and SIS [B] biomaterials at selective stages of repair. For all images, respective marker expression is labeled in red (Alexa Fluor 647 labeling) or green (Alexa Fluor 488 labeling) with blue DAPI nuclear counterstain. Scale bars for all panels = 200 μm. [**C-G**] Histomorphometric assessments of marker expression in specimens

described in [A-B]. N=3-5 rats per group were assessed per data point. Data are displayed as means ± SD. Results from all groups were evaluated with Kruskal–Wallis and post hoc Dunn's tests. (*) = $p<0.05$ compared to NSC. (#) = $p<0.05$ compared to respective 1 week timepoint.

Figure 5. Breeding and live birth evaluations in implant groups. [**A**] Representative photomicrograph of a pregnant rat exhibiting abdominal distension and breast development following vaginal repair with a BLSF graft. [**B**] Live neonatal rat pups delivered from rats described in [A]. [**C**] Quantitation of live births from each implant group. N=4 per data point. Data are displayed as means ± SD. Results were analyzed with the Mann–Whitney U test yielding $p=0.89$.

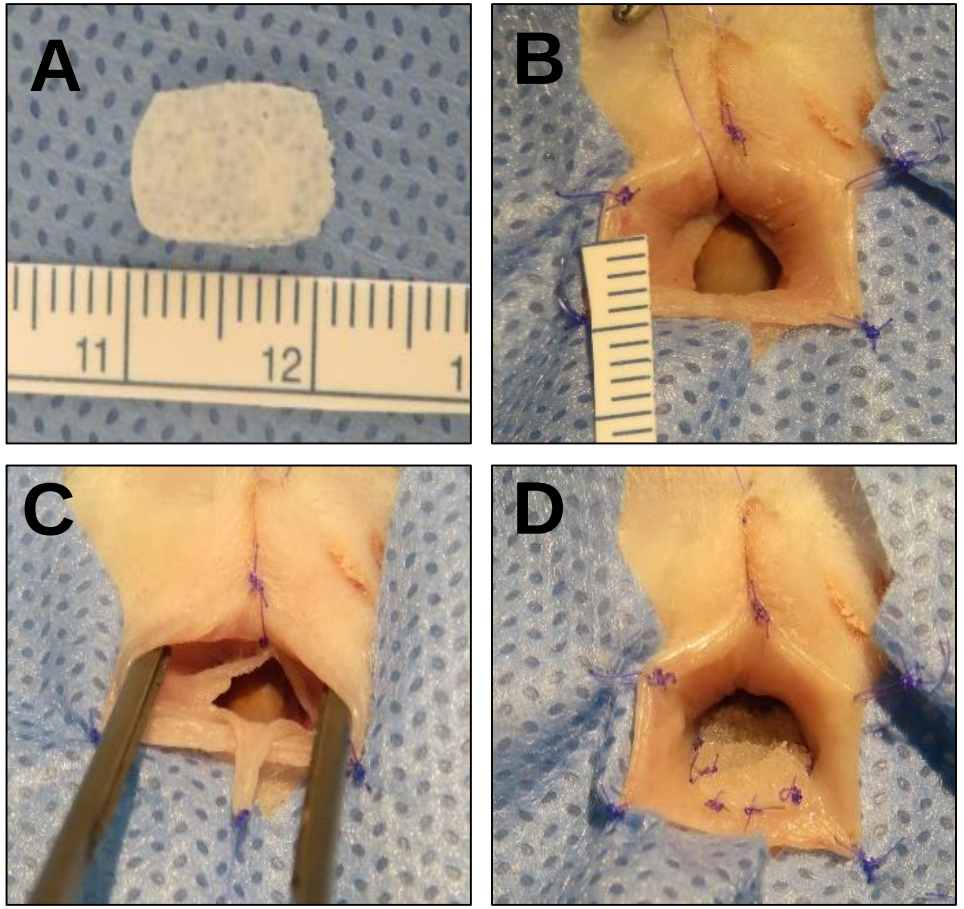

Figure 1

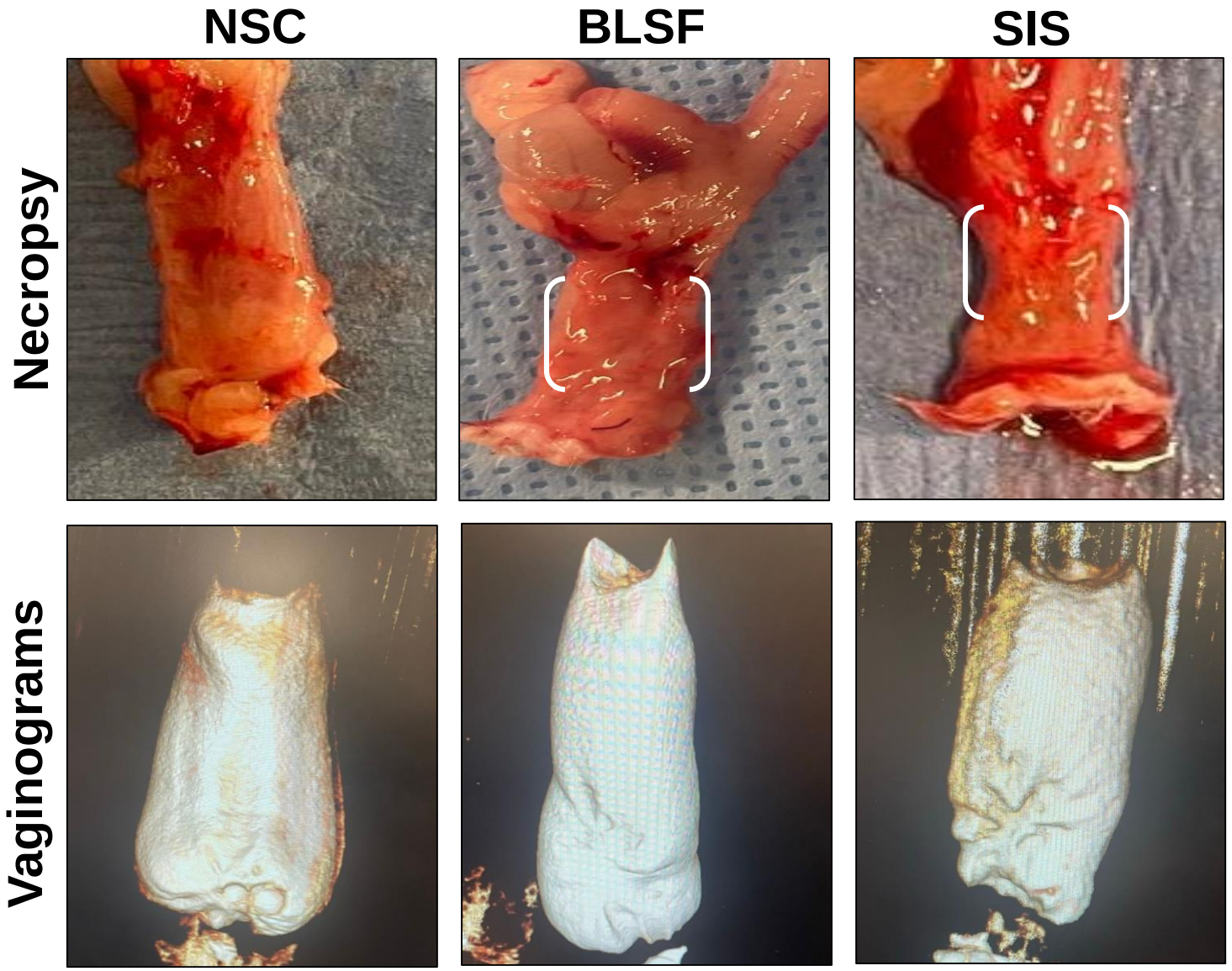

Figure 2

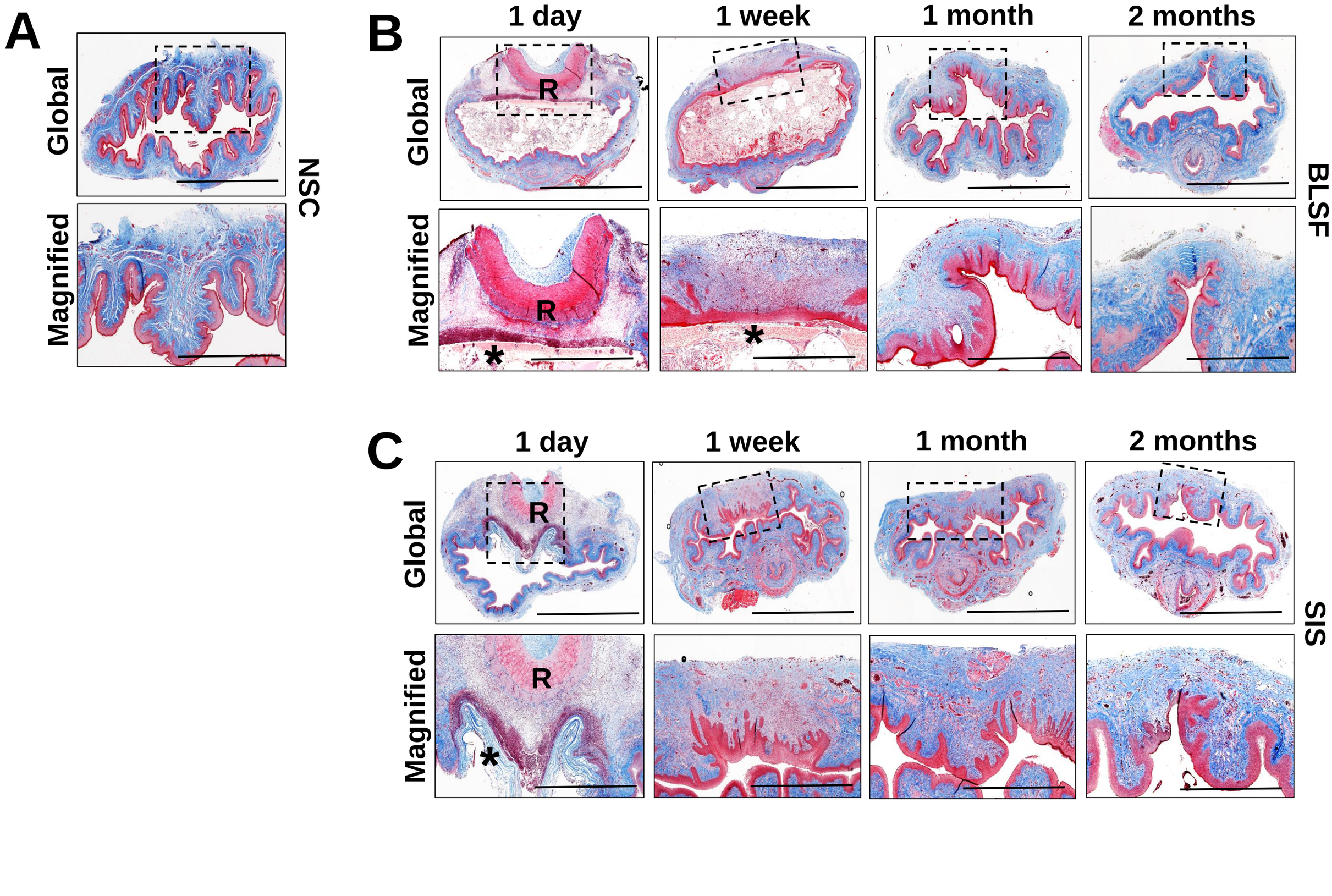
A
Global
Magnified
NSC
B
1 day
1 week
1 month
2 months
Global
Magnified
R
*
BLSF
C
1 day
1 week
1 month
2 months
Global
Magnified
R
*
SIS
D
Collagen Content
NSC BLSF SIS
Relative Immunoreactivity
150
100
50
0
*
#
#
NSC
1 Week
1 Month
2 Months

Figure 3

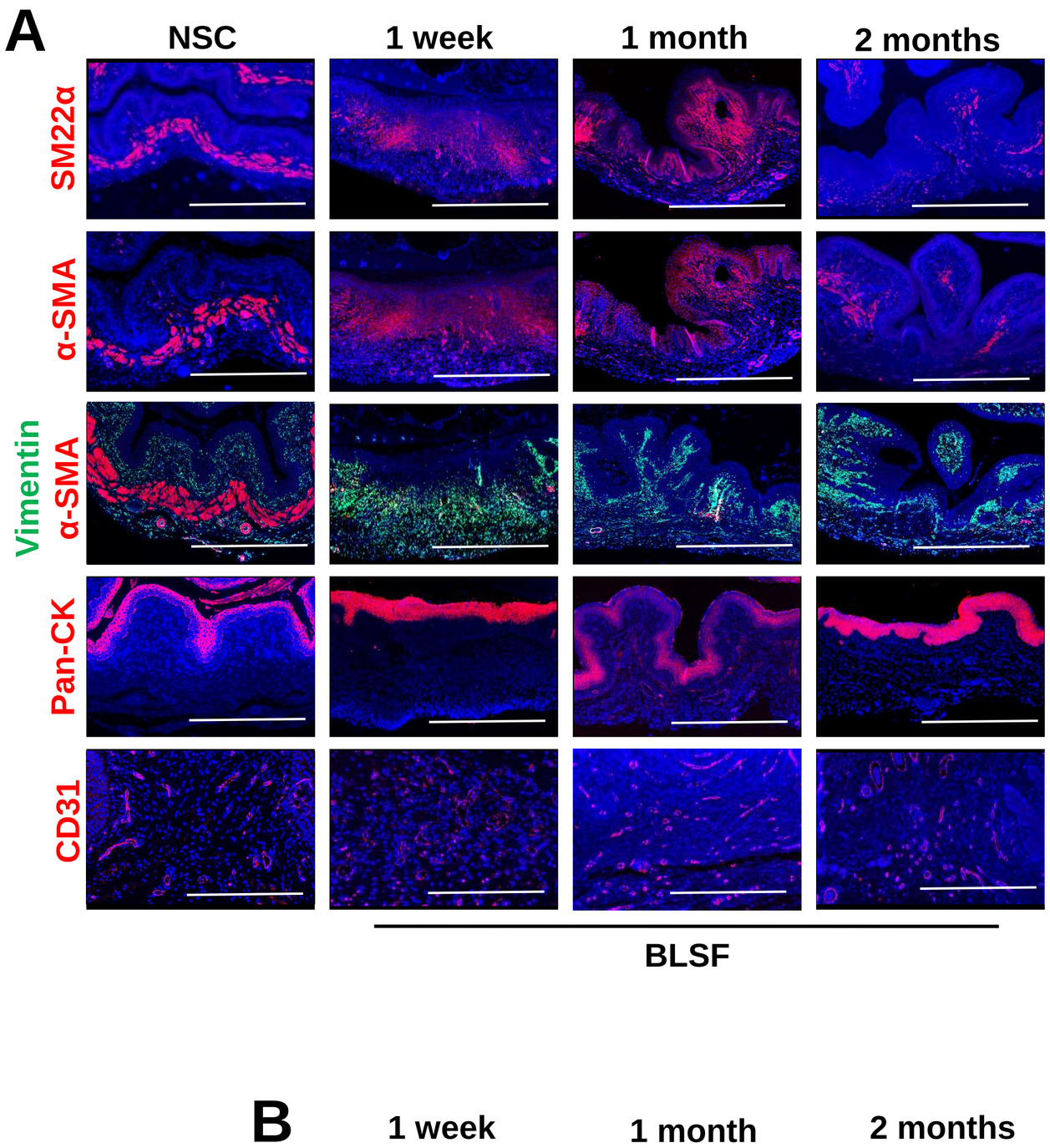
A
NSC
1 week
1 month
2 months
SM22α
α-SMA
Vimentin
α-SMA
Pan-CK
CD31
BLSF

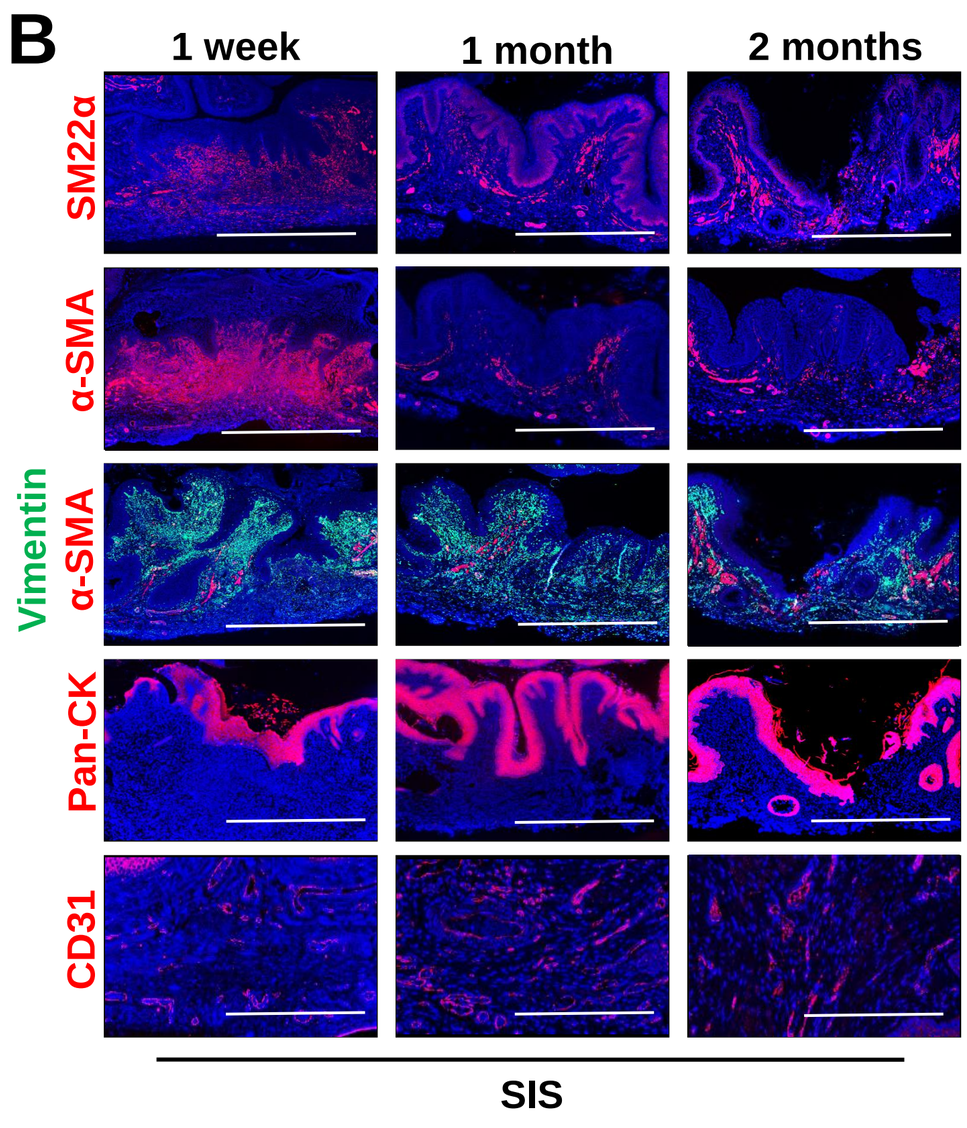
B
1 week
1 month
2 months
SM22α
α-SMA
Vimentin
α-SMA
Pan-CK
CD31
SIS

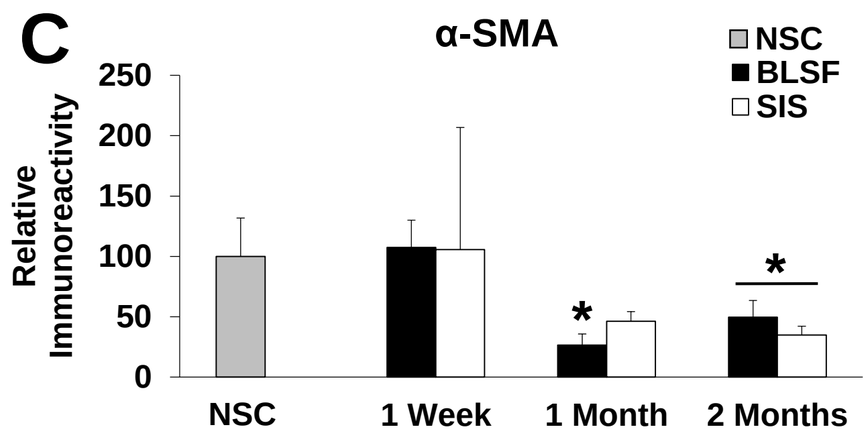
C
α-SMA
NSC
BLSF
SIS
Relative Immunoreactivity
250
200
150
100
50
0
*
*
NSC
1 Week
1 Month
2 Months

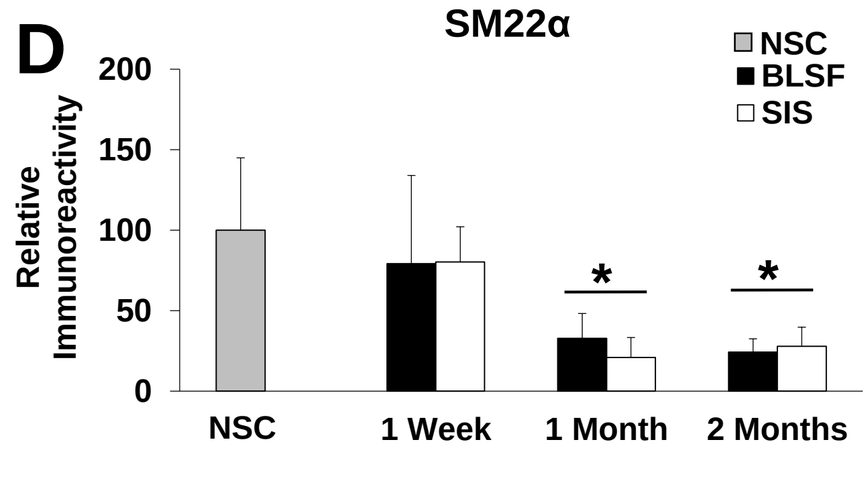
D
SM22α
NSC
BLSF
SIS
Relative Immunoreactivity
200
150
100
50
0
*
*
NSC
1 Week
1 Month
2 Months

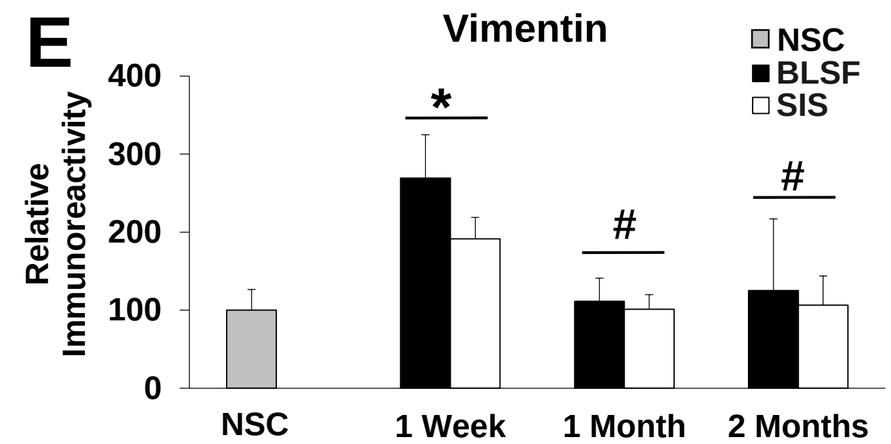
E
Vimentin
NSC
BLSF
SIS
Relative Immunoreactivity
400
300
200
100
0
*
#
#
NSC
1 Week
1 Month
2 Months

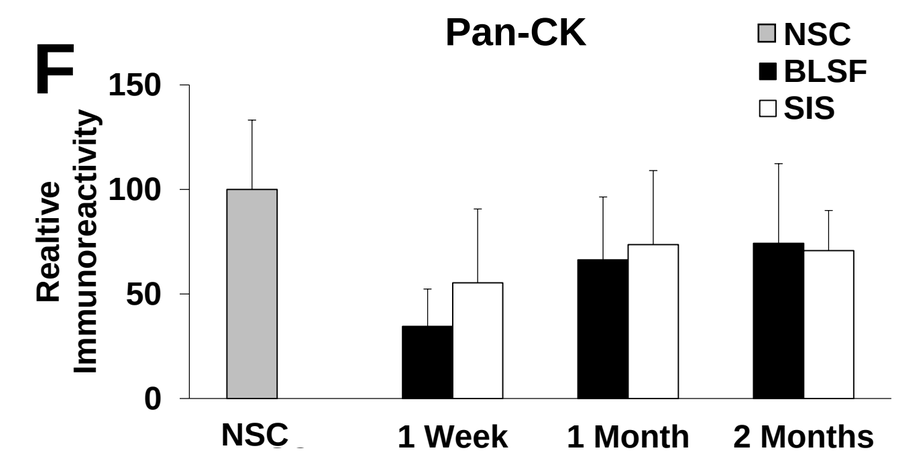
F
Pan-CK
NSC
BLSF
SIS
Realtive Immunoreactivity
150
100
50
0
NSC
1 Week
1 Month
2 Months

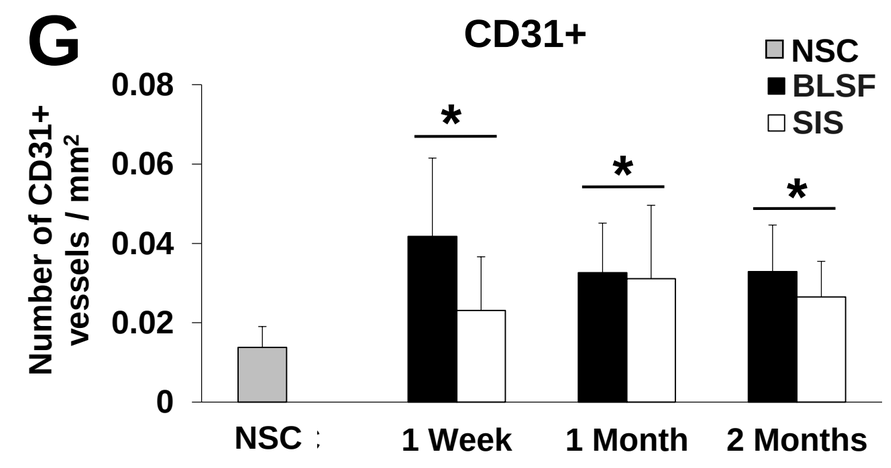
G
CD31+
NSC
BLSF
SIS
Number of CD31+ vessels / mm²
0.08
0.06
0.04
0.02
0
*
*
*
NSC
1 Week
1 Month
2 Months

Figure 4

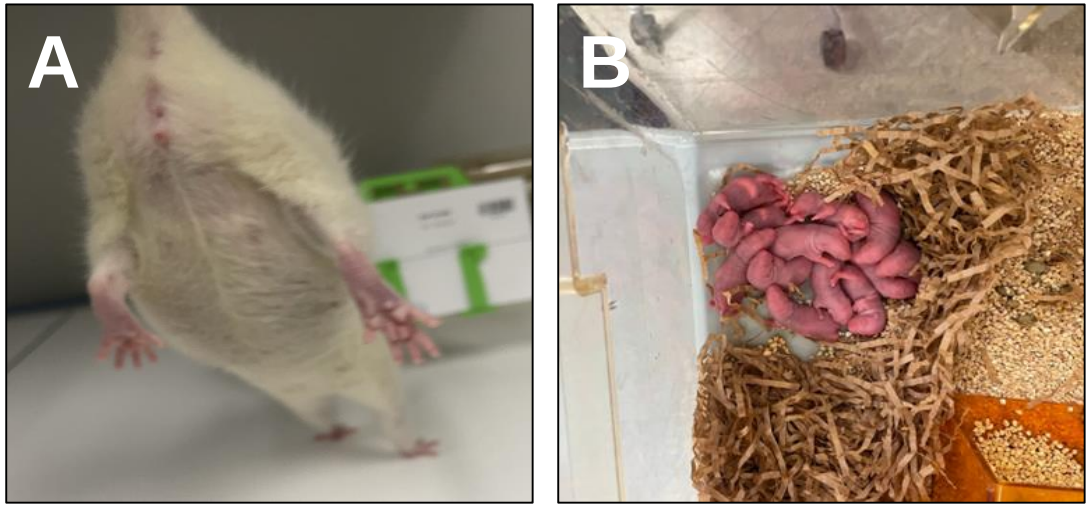
A
B

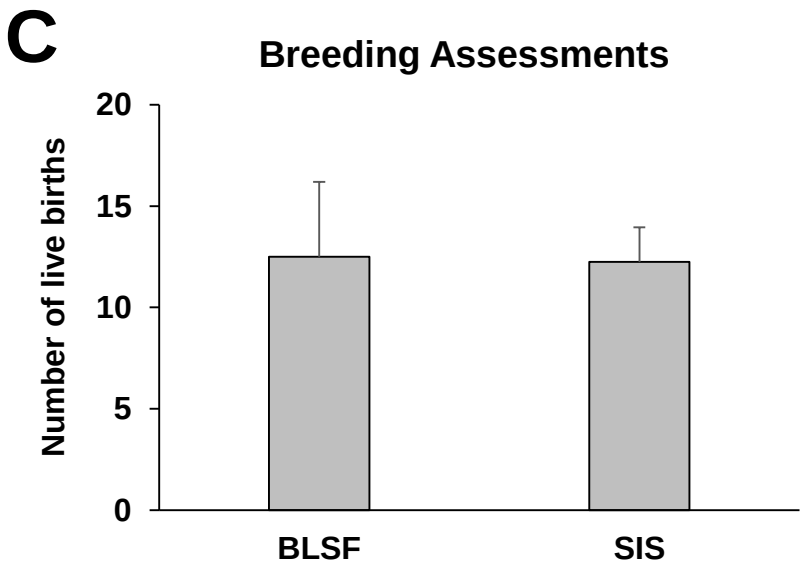
C
Breeding Assessments
Number of live births
20
15
10
5
0
BLSF
SIS

Figure 5